Effect of nickel doping on the structure, morphology and oxygen evolution reaction performance of Cu-BTC derived $CuCoO_2$

Miao Yang,[a,b] Na Han,[b] Lifen Shi,[b] Han Gao,[a] Xing Liu,[a] Yue Mi,[a] Xianwei Zeng,[c] Jilin Bai [a] and Dehua Xiong[,a,b]*

a. State Key Laboratory of Silicate Materials for Architectures, Wuhan University of Technology, Wuhan 430070, P. R. China.

b. State Key Laboratory of Advanced Technology for Float Glass, CNBM Research Institute for Advanced Glass Materials Group Co., Ltd., Bengbu 233017, P. R. China.

c. Zhejiang Kelei New Material Co., Ltd., Huzhou 313300, P. R. China.

* Corresponding author email: xiongdehua2010@gmail.com

Experimental Details

Materials synthesis

All of the chemicals in these experiments were purchased from Sinopharm Chemical Reagent Co., Ltd with an analytical grade and used as received. Delafossite $CuCoO_2$ crystals with different Ni dopants were prepared through a modified hydrothermal method, according to our previous works. Specifically, 0.55 mmol $Co(NO_3)_2 \cdot 6H_2O$, 0.55 mmol $Cu(NO_3)_2 \cdot 3H_2O$, 0.55x mmol $NiCl_2 \cdot 6H_2O$ (x =0, 0.01, 0.03 and 0.05, marked as CCO, 1NCCO, 3NCCO and 5NCCO) and 0.20 g CuBTC, were mixed together in the mixed solution of 20 ml deionized (DI) water and 50ml ethanol. 5.40 g NaOH was subsequently added to the above solution, and the precursor solution was stirred for a few hours at room temperature. Afterwards, the turbid solution was sealed in a 100 mL Teflon-lined autoclave and was heated to 140 ℃ for 24 hours. The as-synthesized powder was washed with aqueous ammonia solution, deionized water and ethanol in turn for several times, and was collected by a centrifuging method. Finally, the powder sample was dried at 70 ℃ for 5 hours for further characterization.

Structural characterization

The crystal phase of samples was characterized by the powder X-ray diffraction (XRD, D8 Advance). The morphology, microstructure, and chemical composition of the samples were examined by field-emission scanning electron microscopy (FESEM, S4800, produced by Hitachi, Japan) and transmission electron microscopy (TEM, JEOL JEM-2100 operating at 200 keV) equipped with energy-dispersive X-ray spectroscopy (EDX). The surface chemical states of $CuCoO_2$-based powders and Ni@5NCCO working electrodes were analyzed by X-ray photoelectron spectroscopy (XPS, Thermo Escalab 250Xi). XPS measurements were performed at a 01 emission angle using an Al Kα radiator (Ephoton = 1486.6 eV) with a filament current of 10 mA and a filament voltage energy of 14.7 keV. To compensate for the charging of the sample, a charge neutralizer is used. The C 1s line (284.80 eV) corresponding to the surface adventitious carbon (C-C line bond) has been used as the reference binding energy. The Brunauer-

Emmett-Teller (BET) specific surface areas and porosity parameters of the samples were taken by N_2 adsorption-desorption isothermetry (Micromeritics TriStar II 3020 3.02). The particle size distribution of the samples was determined by nanoparticle size and zeta potential analyzer (Zeta ZS90 & Mastersizer 3000). The element proportion of the samples was analyzed by inductively coupled plasma-atomic emission spectrometry (ICP-AES, Prodigy 7).

Electrode preparation and electrochemical measurement

The OER performance was evaluated by cyclic voltammetry (CV) and electrochemical impedance spectroscopy (EIS) in a three-electrode configuration in 1.0 M KOH (pH = 13.5) using a CS2350H electrochemical workstation (Wuhan Corrtest Instruments Corp., China). A platinum wire and a saturated calomel electrode (SCE) were used as the counter and reference electrodes, respectively. To prepare the nickel (Ni) foam supported CCO and xNCCO based NSs (Ni@CCO and Ni@xNCCO, x=1, 3, and 5.) working electrodes, 15 mg Ni-doped or pure $CuCoO_2$ powders were dispersed in a mixture of 500 μL water, 480 μL isopropanol and 20 μL Nafion (5 wt%, Sigma). 20 μL suspension was then drop cast on to the surface of the Ni foam sheets (surface area: 1.0 cm^2), and the working electrode was dried at 150 ℃ for 10 minutes. The loading mass of these working electrode was kept at 0.30 $mg \cdot cm^{-2}$. Cyclic voltammetric (CV) scans were recorded between 1.05 and 1.80 V vs. reversible hydrogen electrode (RHE) at a scan rate of 5 $mV \cdot s^{-1}$. The electrochemical double-layer capacitance (C_{dl}) can be extracted through CV scans recorded at different rates (from 20 to 100 $mV \cdot s^{-1}$) in the non-faradaic potential window of -0.05-0.05 V vs. SCE. The EIS measurements were performed in the frequency range of 100 kHz-10 mHz under a constant potential of 1.63 V vs. RHE.

All current density values are normalized with respect to the geometrical surface area of the working electrode. All CV curves presented in this work are iR-corrected (85%). The correction was done according to the following equation:

$$E_c = E_m - iR_s \quad (1)$$

where E_c is the iR-corrected potential, E_m experimentally measured potential, and R_s the equivalent series resistance extracted from the electrochemical impedance spectroscopy measurements. Unless otherwise specified, all potentials are reported versus reversible hydrogen electrode (RHE) by converting the potentials measured vs. SCE according to the following formula:

$$E\ (RHE) = E\ (SCE) + 0.241 + 0.059\ pH \qquad (2)$$

Supplementary tables:

Table S1. The calculated element proportion of CCO, 1NCCO, 3NCCO and 5NCCO from ICP-AES results.

Samples	Cu/Co %	Ni/(Ni+Co) %
CCO	100.0	-
1NCCO	117.0	1.2
3NCCO	115.5	2.9
5NCCO	106.9	3.9

Supplementary figures:

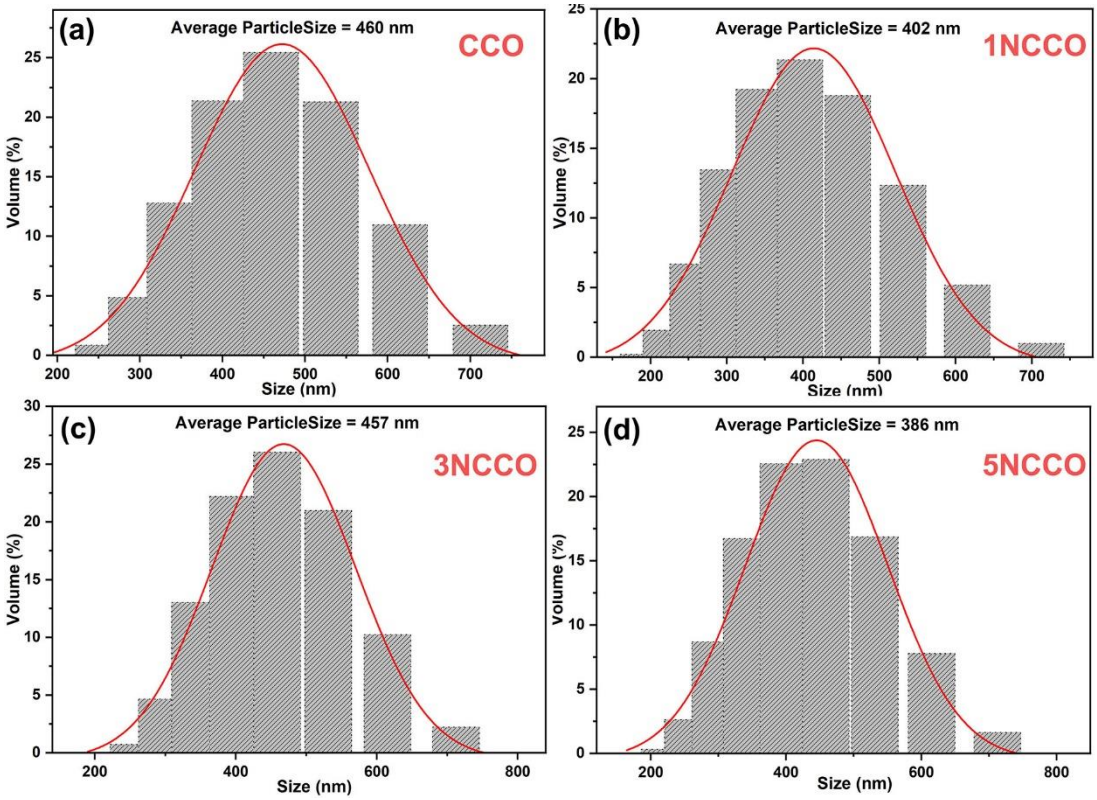

Fig. S1. The particle size distribution of CCO (a), 1NCCO(b), 3NCCO(c) and 5NCCO (d) samples.

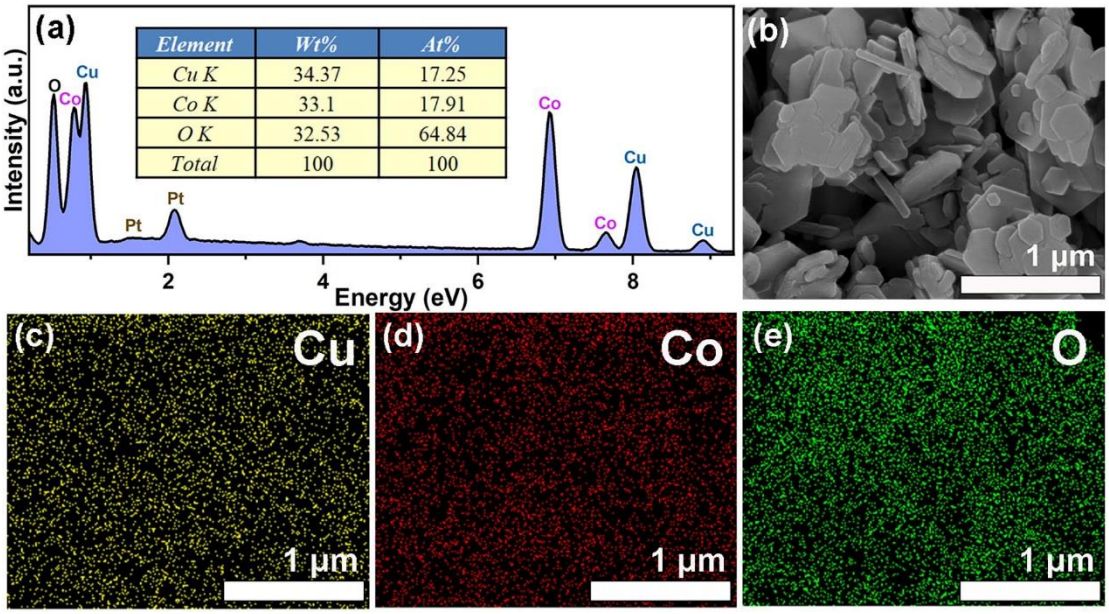

Fig. S2. EDX spectrum (a), SEM images (b) and elemental maps (c-e) of CCO powder.

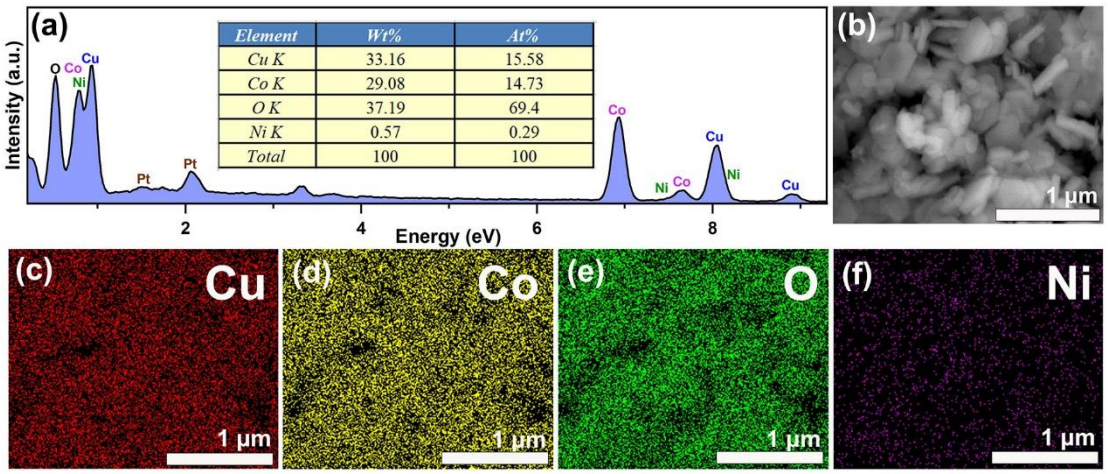

Fig. S3. EDX spectrum (a), SEM images (b) and elemental maps (c-e) of 1NCCO powder.

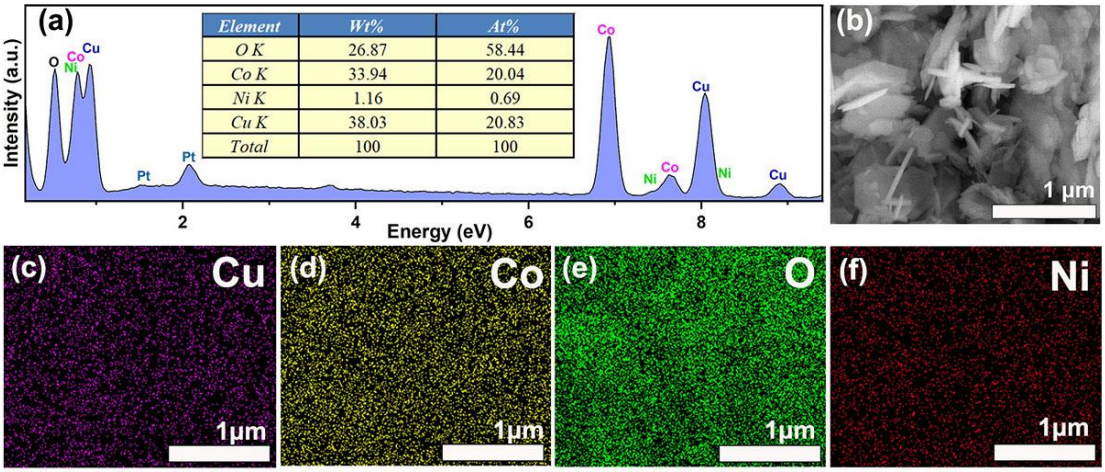

Fig. S4. EDX spectrum (a), SEM images (b) and elemental maps (c-e) of 3NCCO powder.

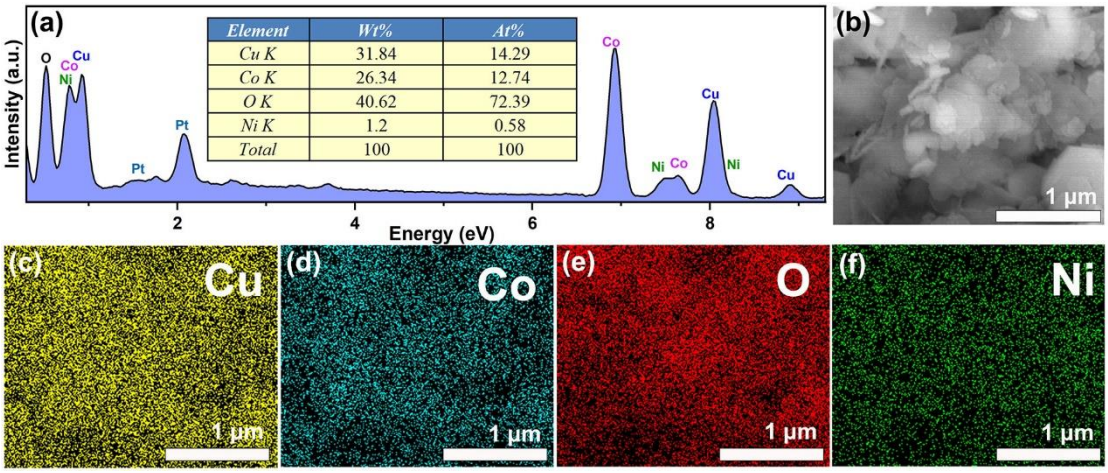

Fig. S5. EDX spectrum (a), SEM images (b) and elemental maps (c-e) of 5NCCO powder.

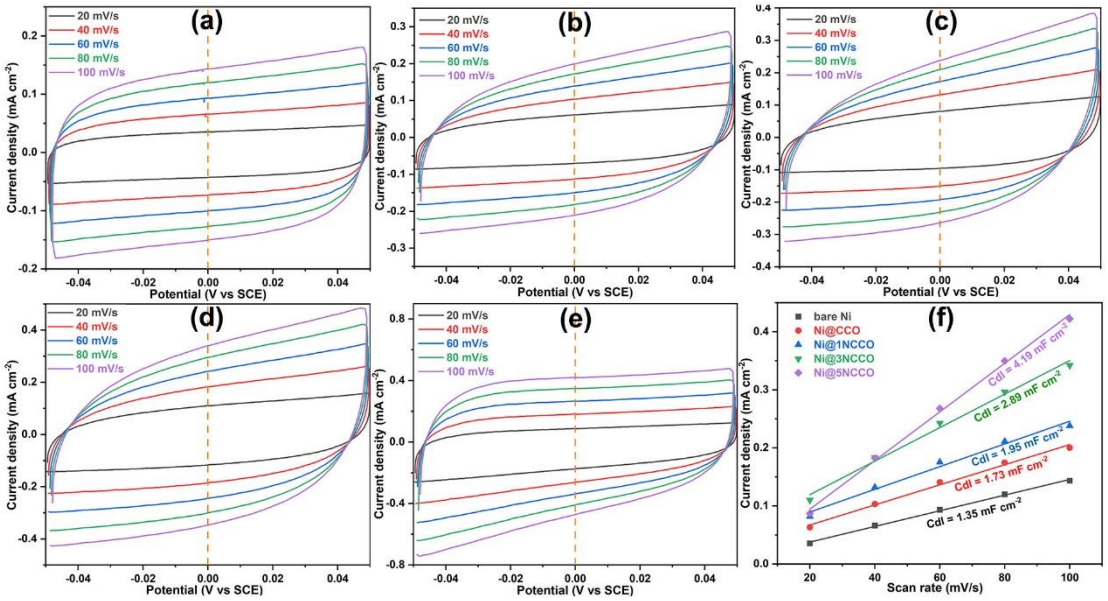

Fig. S6. CV curves at the scan rates from 20 to 100 mV s^{-1} of bare Ni (a), Ni@CCO (b), Ni@1NCCO (c), Ni@3NCCO (d)and Ni@5NCCO (e) measured in the non-Faradaic region, and the calculated double-layer capacitance C_{dl} (f) of these CCO based samples.

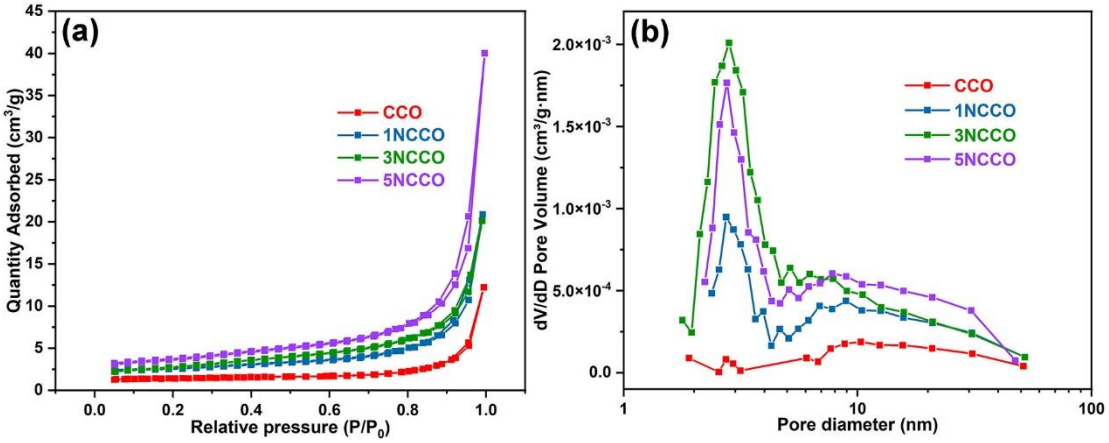

Fig. S7. N_2 adsorption-desorption isotherms(a) and pore structure(b) of CCO, 1NCCO, 3NCCO and 5NCCO powders.